

Investigating ultrafast two-pulse experiments on single DNQDI fluorophore: a stochastic quantum approach[†]

Giulia Dall'Osto,^a Emanuele Coccia,^b Ciro A. Guido,^a and Stefano Corni^{ac‡}

^a Department of Chemical Sciences, University of Padova, via Marzolo 1, Padova, Italy

^b Department of Chemical and Pharmaceutical Sciences, University of Trieste, via Giorgieri 1, Trieste, Italy

^c CNR Institute of Nanoscience, via Campi 213/A, Modena, Italy

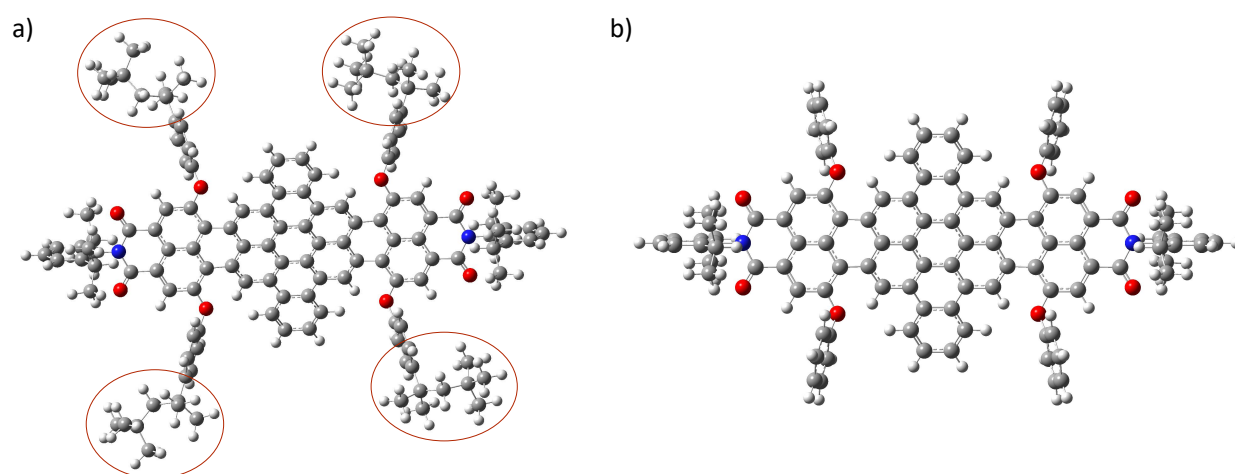


Figure S1: a) Full and b) reduced model of DNQDI molecule. Circles in (a) show the alkylic chains eliminated to build the reduced model.

Comparison between Lindblad master equation and SSE results

The SSE results for a vibronic dynamics (obtained averaging 100 or 200 trajectories) were compared with the Lindblad equation ones (Figure S2). Density matrix propagation of the system was performed solving ordinary differential equation with Dormand-Prince method already implemented in Matlab-R2018b (ode45).¹⁻³ The results obtained with 200 trajectories are in agreement with density matrix results but also with 100 trajectories the results are quite good and the oscillatory behaviour of population as the decay rate are well-distinguished. The ratio between the errors with 100 and 200 trajectories is about $\sqrt{2}$.

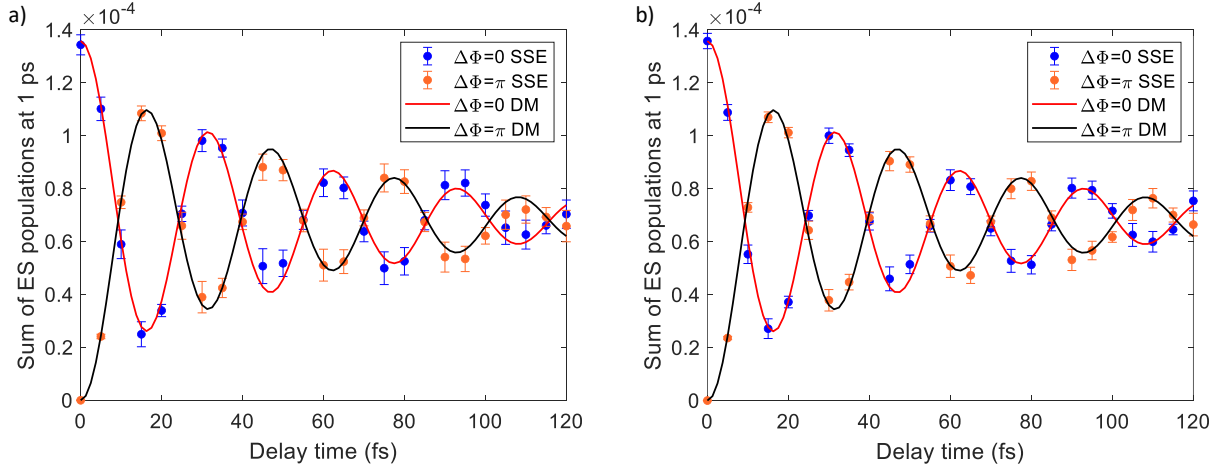


Figure S2: Comparison between sum of excited-state populations at the end of simulation as a function of delay time between density matrix approach (DM) and (a) 100 SSE trajectory or (b) 200 SSE trajectories. $\Delta\phi = 0, \pi$ have been considered and a field with FWHM = 15 fs, $I_{max} = 1 \times 10^9$ W/cm². One normal mode was added to the system description.

Real-time simulations including 5 electronic excited states

In order to verify that in the experimental condition higher-energy electronic states are not involved in the dynamics we have considered a wave function obtained as linear combination of 6 electronic states (5 excited states have been calculated at tddft/B3LYP level of theory, see table S1) for the reduced model of the molecule. The electronic dynamics has been computed under the experimental conditions reported in the main text. The sum of populations of the 5 excited states (panel b) of figure S3) coincides with that of only the first excited state (panel a) of figure S3).

Table S1: Excitation energy at TDDFT/B3LYP level of theory

Excited state	Energy (eV)
1	1.7572
2	2.2646
3	2.4139
4	2.6455
5	2.8697

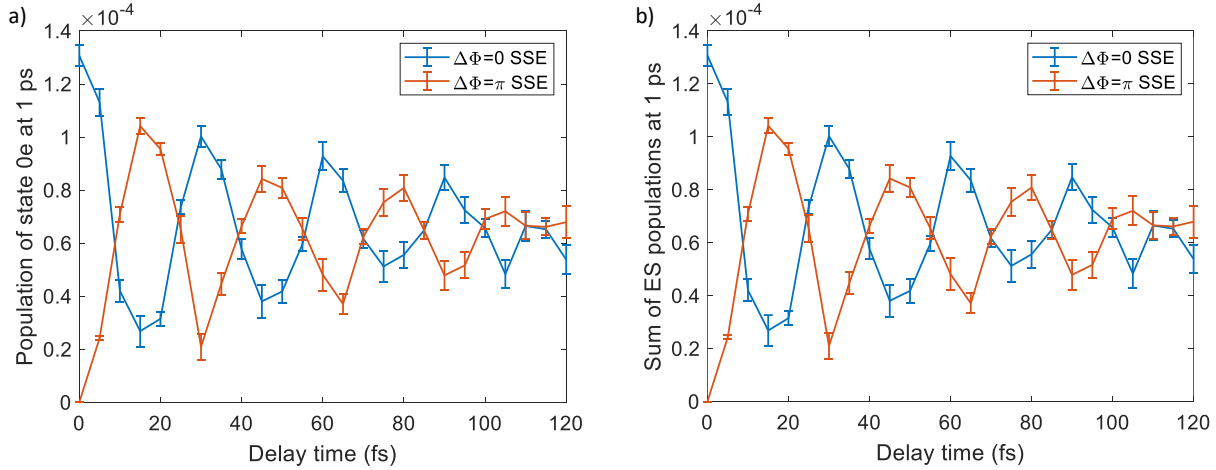


Figure S3: a) Population of first excited state at the end of dynamics as a function of delay time, b) sum of excited state population at the end of dynamics as a function of delay time.

Two-photon processes

We have calculated higher-energy excitations, up to around 3.6 eV, to verify the absence of two-photon processes in the simulations carried out in the experimental conditions. TDDFT/B3LYP calculations have been performed including 40 excited states, and the transition dipole moments between excited states have been calculated through TDDFT/B3LYP within the Tamm-Dancoff approximation. The results of the two approaches have been compared exploring the metrics of the electronic transitions^{4,5} on the basis of Natural Transition orbitals.⁶ Table S2 reports excited-state energy within the range 3.40 – 3.62 eV (around twice the value of the first electronic state excitation energy) computed with the two methods, the energy difference and the transition dipole moments $\vec{\mu}_{1n}$ from the first excited state. As the results point out, two-photon processes can be neglected in our study (and thus also higher energy excited states) since transition dipole moments are very small and consequently also the excitation probabilities.

Table S2: Excitation energy at TDDFT/B3LYP level of theory without ('Energy') and within ('Energy TDA') the TDA, excitation energy differences between the two methods and transition dipole moments from the first excited state. Only the states with an energy in the range relevant for possible two-photon absorption are given.

Excited state (n)	Energy (eV)	Energy TDA (eV)	Energy difference (eV)	μ_{1n}
22	3.4059	3.4219	0.016	0.5693
23	3.4307	3.4365	0.0058	0.0001
24	3.4324	3.4383	0.0059	0.0000
25	3.4453	3.4594	0.0141	0.0002
26	3.484	3.5078	0.0238	0.0000
27	3.4958	3.5163	0.0205	0.0002
28	3.5425	3.5427	0.0002	0.0294
29	3.5445	3.5447	0.0002	0.0001
30	3.5798	3.5938	0.014	0.0001
31	3.6119	3.6174	0.0055	0.0000
32	3.6123	3.6192	0.0069	0.0001

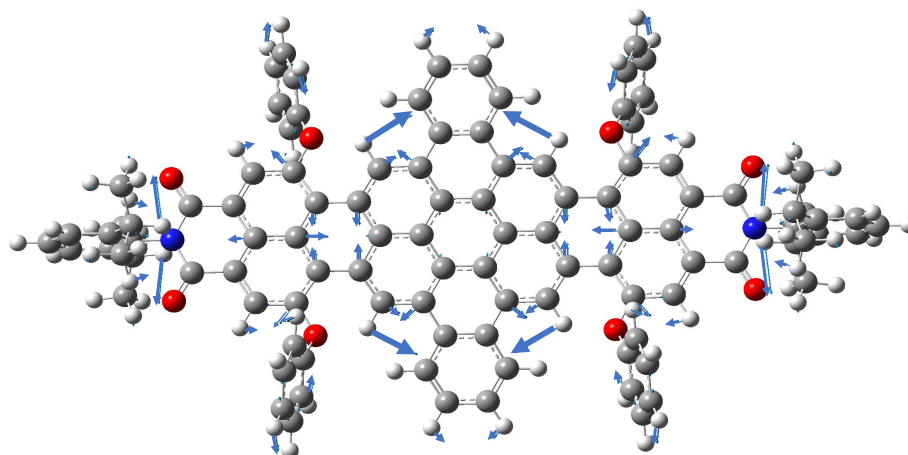


Figure S4: Snapshot of normal mode NM1 (1368 cm^{-1}) in reduced model of DNQDI.

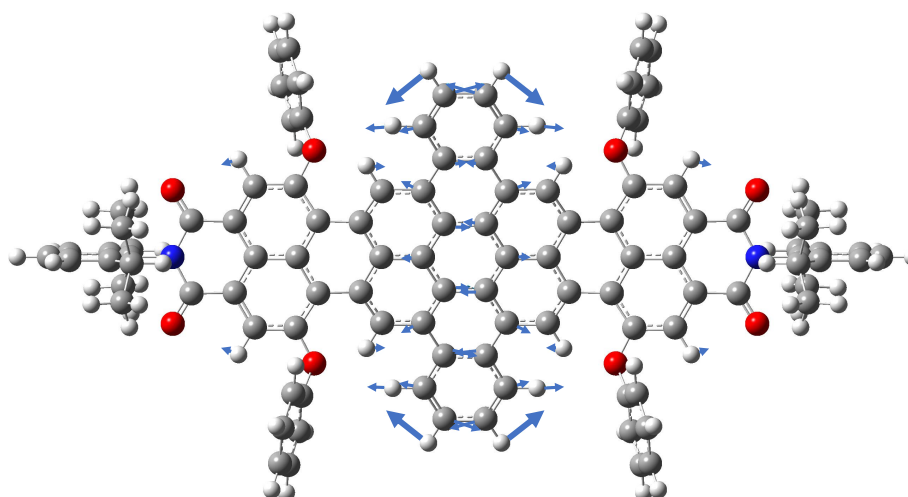


Figure S5: Snapshot of normal mode NM2 (1629 cm^{-1}) in reduced model of DNQDI.

Real-time simulations with a different detuning

We also considered a detuning of 626 cm^{-1} (Figures S6, S7 and S8). This detuning corresponds to the shift between the pulse frequency and the maximum absorption energy (507 cm^{-1}) experimentally employed, plus the energy difference between the maximum of the absorption spectrum simulated and the $|0_g\rangle - |0_e\rangle$ energy (119 cm^{-1}). Pulses are characterized by a Gaussian envelope function, with FWHM equal to 15 fs and maximum intensity of the electric field $I_{max} = 1 \times 10^9 \text{ W/cm}^2$. T_1 and T_2 values are same mentioned in the

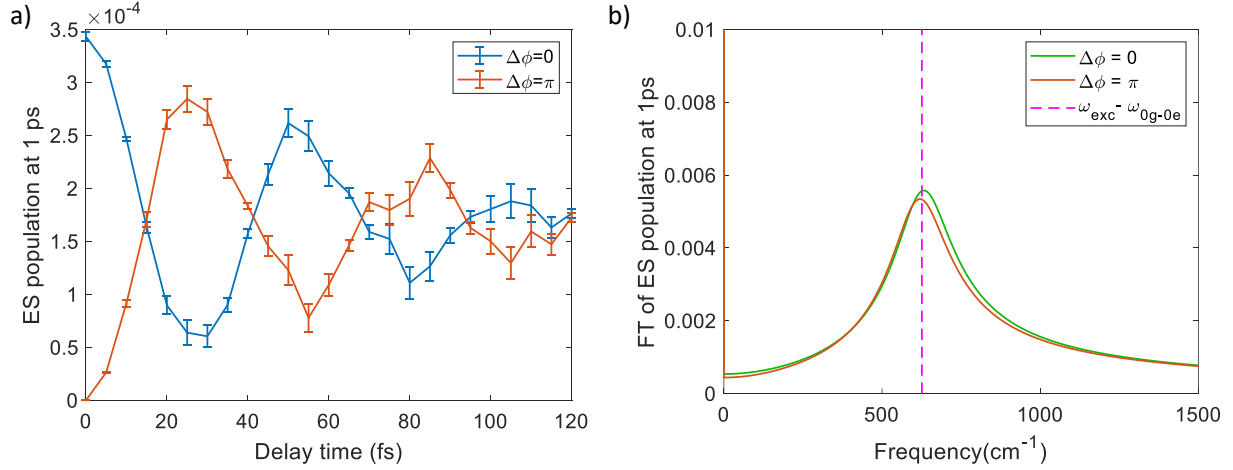


Figure S6: a) Electronic dynamics of a pure electronic two-level system, equivalent to figure 4 in the main text. b) FT of (a) which reveals the detuning frequency.

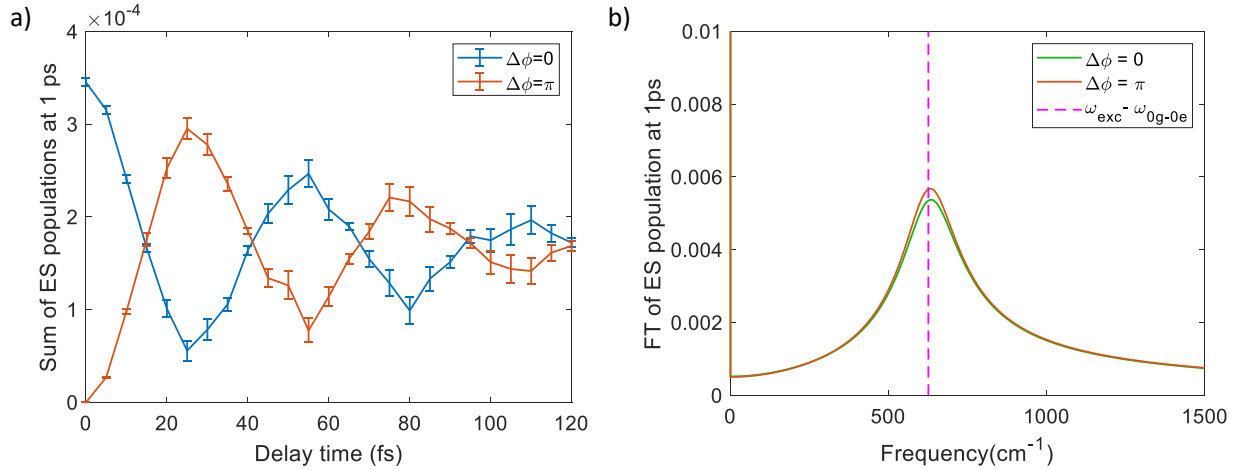


Figure S7: a) Vibronic dynamics of a system with 2 electronic states and 16 vibronic states each, equivalent to figure 6 in the main text. b) FT of (a) which reveals the detuning frequency between pulse frequency ω_{exc} and excitation frequency $|0_g\rangle - |0_e\rangle$. Two normal modes NM1 and NM2 have been considered to compute the vibronic structure.

main text.

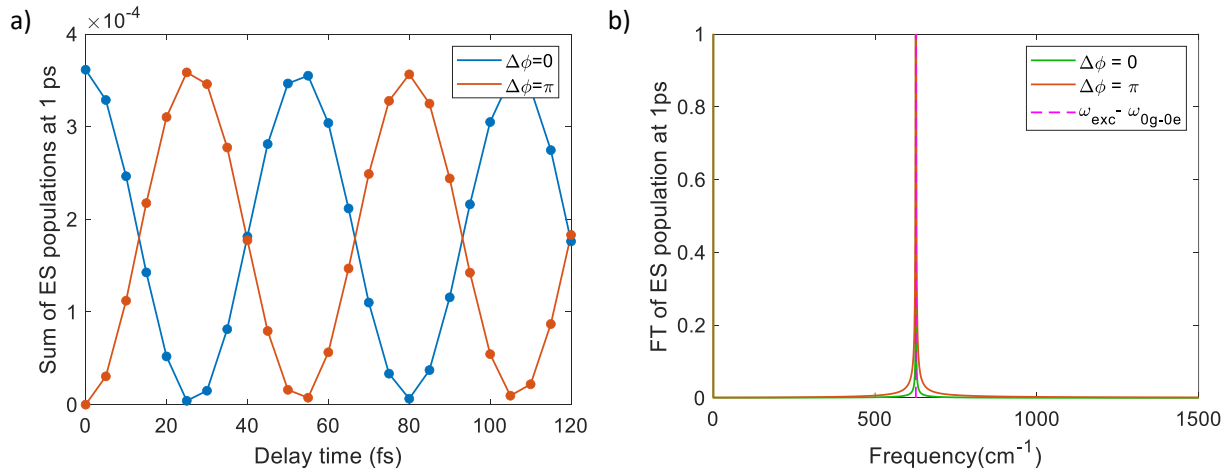


Figure S8: a) Vibronic dynamics of a system with 2 electronic states and 8 vibronic states each, equivalent to figure 8 in the main text. Dephasing has not been included and the pulses are centred at two main frequencies (726 nm and 662 nm), as the experimental pulses. b) FT of (a) which reveals oscillation with detuning frequency between pulse frequency $\omega_{\text{exc}1}$ and excitation frequency $|0_g\rangle - |0_e\rangle$. Only the normal mode NM1 has been considered to compute the vibronic structure.

Electric field shape employed in sec. 4.3.4

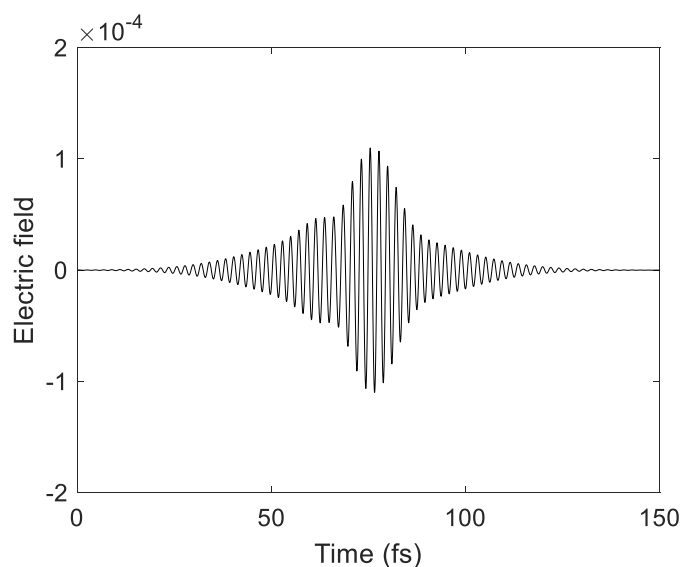


Figure S9: Time profile of the pulse as a convolution of two Gaussian sinusoidal functions (see the main text sec. 4.3.4 for details) .

High field intensity: exclusion of state $|1_g\rangle$

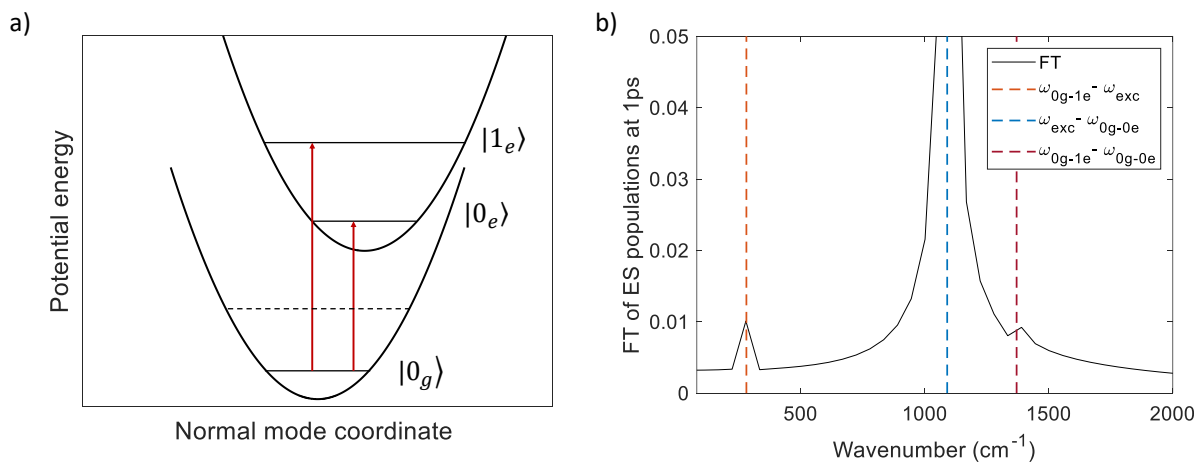


Figure S10: a) Vibronic structure of a three-level system with 2 vibronic states in the electronic excited state. Dephasing has not been included in the simulation. b) FT of excited state populations at 1 ps as a function of delay time. FT reveals the detuning frequency between pulse frequency ω_{exc} and excitation energy of states $|0_e\rangle$ and $|1_e\rangle$.

Ensemble average

In ensemble measurements each molecule experiences a different surrounding environment that slightly affects its geometry, excitation energy and dipole moments producing signal decay that are not related to pure dephasing. Outcomes of ensemble measurements have been simulated (Figure S11) changing the pulse frequency and propagating the same wave packet (with four vibronic states) representing the propagation of different systems exposed to the same electric field. In this case the wave function has been propagate with

the Schrödinger equation without including the stochastic terms (e.g. dephasing and relaxation operators). The sum of excited-state populations at the end of dynamics is weighted by a Gaussian function centred in the most probable excitation frequency and with amplitude equal to dephasing rate (e.g. $1/60 \text{ fs}^{-1}$).

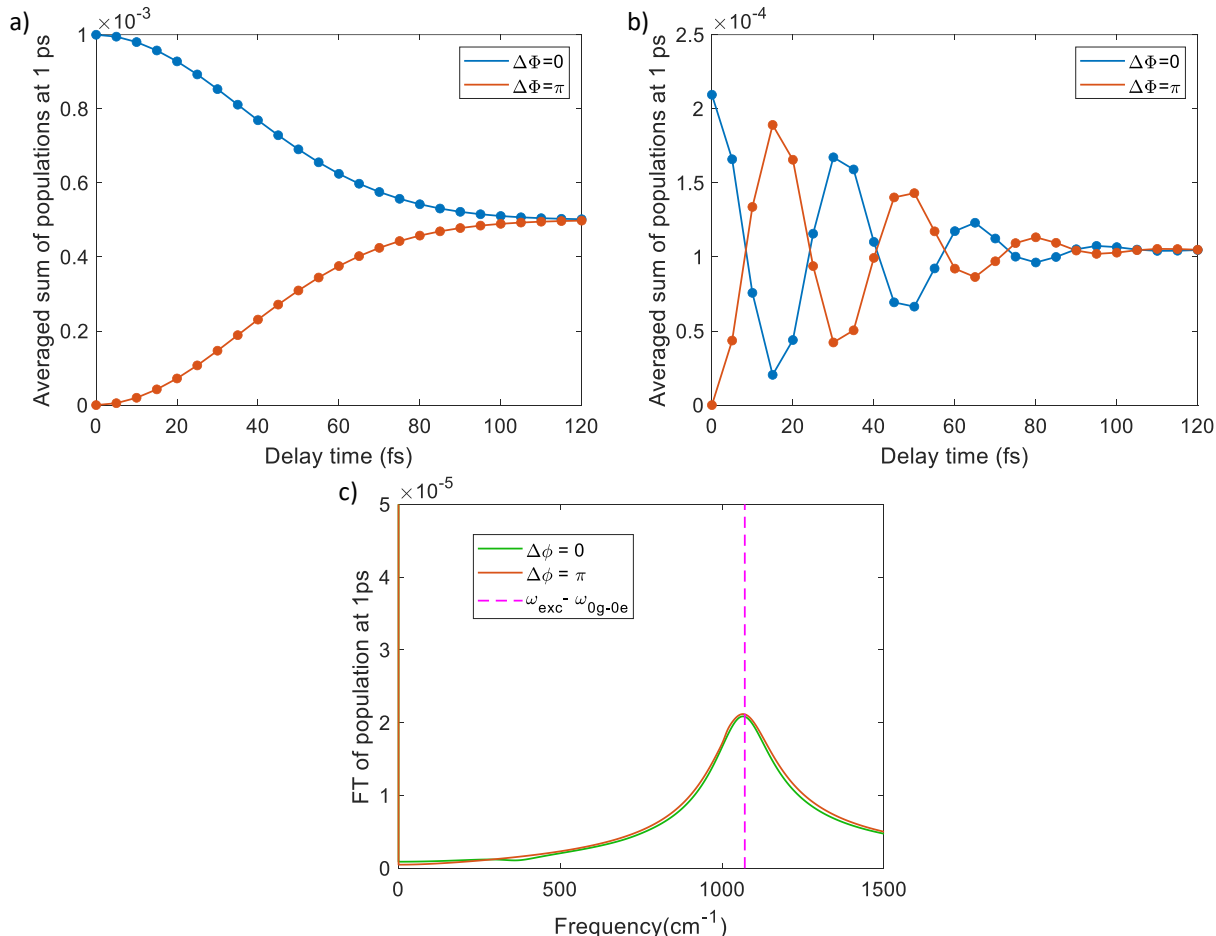


Figure S11: Average of sum of excited-state populations as a function of delay time weighted by a Gaussian function centred in the transition $|0_g\rangle - |0_e\rangle$ frequency (a) and centred in a frequency 1090 cm^{-1} greater than $|0_g\rangle - |0_e\rangle$ transition frequency (b). (c) FT of (b).

Results in figure S11 give evidence that ensemble measurements can lead to a signal decay that do not depends on dephasing, but rather to inhomogeneity experienced by each molecule. For this reason single-molecule techniques are very useful to provide information on the system dynamics avoiding artefacts.

References

- [1] J. R. Dormand and P. J. Prince, *Journal of Computational and Applied Mathematics*, 1980, **6**, 19–26.
- [2] L. F. Shampine, *Numerical Solution of Ordinary Differential Equations* Chapman & Hall New York, 1994.
- [3] P. Bogacki and L. F. Shampine, *Applied Mathematics Letters*, 1989, **2**, 321–325.
- [4] C. A. Guido, P. Cortona, B. Mennucci and C. Adamo, *Journal of Chemical Theory and Computation*, 2013, **9**, 3118–3126.
- [5] C. A. Guido, P. Cortona and C. Adamo, *The Journal of chemical physics*, 2014, **140**, 104101.
- [6] R. L. Martin, *The Journal of chemical physics*, 2003, **118**, 4775–4777.